Supplementary Information

Optimal design of decentralized ammonia production via electric Haber–Bosch

Authors: Lorenzo Rosa* and Davide Tonelli

Affiliation:
Biosphere Sciences & Engineering, Carnegie Institution for Science, Stanford, CA 94305, United States of America

Corresponding Author:
*Lorenzo Rosa, lrosa@carnegiescience.edu

Table of Contents

S1. Cost of capital

The cost of capital is derived based on (Damodaran, 2023), under the assumption that 100% of the capital invested for the installation of a plant derives from equity, whose risk depends on country-specific equity and sector-specific risk premiums. The selected sector of reference for the selection of the risk premium is renewable technologies, since part of the equipment involved is renewable technologies, and the deployment of a small-scale decentralized electric Haber-Bosch system is part of decarbonization strategies.

S1.1 Method of estimation

The cost of capital, r, is computed as the total equity risk premium of an asset in a specific country based on the capital asset pricing model:

$$r = R^f + R^p = R^f + ß\ R^c \quad \text{(S1)}$$

where:

- R^f: mature equity market risk premium computed as the implied equity risk premium of the S&P500 assumed equal to 4.33% (Damodaran, 2023);
- R^p: country- and sector-specific risk premium;
- R^c: country-specific equity risk premium assuming Moody's sovereign rating measuring the country's default risk (Table S1);
- ß: market-specific relative equity volatility (beta) from historical data of all companies in the green and renewable energy industry within the market region.

S1.2 Country-specific data

Table S1. Data used for cost of capital estimation. Source: (Damodaran, 2025), last update 09/01/2025.

country	Moody's rating	Default risk (R_c)	Beta (ß)	Cost of capital (r)
Brazil	Ba1	2.48%	0.82 (emerging markets)	6.36%
India	Baa3	2.18%	0.82 (emerging markets)	6.11%
China	A1	0.70%	0.82 (emerging markets)	4.90%
United States	Aaa	0.00%	1.13 (United States market)	4.33%
Italy	Baa3	2.18%	0.81 (European market)	6.09%
Ethiopia	Caa2	8.92%	0.82 (emerging markets)	11.64%

S2. System optimization model

The production of ammonia in the electric Haber-Bosch technology involves two reactions, water electrolysis and the ammonia synthesis loop:

$$H_2O \rightarrow H_2 + 0.5\ O_2 \quad \text{(water electrolysis)} \qquad \text{(S2)}$$
$$3\ H_2 + N_2 \rightarrow 2\ NH_3 \quad \text{(ammonia synthesis)}$$

Electricity feeding water electrolysis can either be supplied with the installation of renewable technologies (solar and wind), herein referred as autonomous system, with possible connection to the power grid, herein referred as hybrid system, or solely by the grid, herein referred as grid-connected system.

All the components of the system are modeled and optimized with a mixed integer linear program (MILP) that identifies the optimal sizing and operation of the system components by minimizing the total cost of the system. The model is coded in Python using the Pyomo library and solved with Gurobi Optimizer (version 12.0.3) (Gurobi, 2025).

S2.1 Model formulation

This section details the model formulation used for the optimization of the system to identify the system's design and operation with hourly resolution.

S2.1.1 Sets

- H: set of timesteps in a year;
- $H_s \in H$: set of subsets s in a year which define the timeframes when the 100% supply reliability condition is applied;
- S: set of indices referring to the number of subsets H_s;
- T: set of years within the technology's lifetime.

S2.1.2 Decision variables

Table S2. Decision variables of the optimization model. The table presents the decision variables used in the formulation of the optimization model.

Symbol	Description	Unit	Domain	Definition
Power production technologies				
P_t^{el}	Electricity feeding the system for ammonia production, where "el" refers to "PV", "wind", and "grid" technologies	kWh	R^+	$\forall\, t \in H$
W^{el}	Installed power production capacity where "el" refers to "PV", "wind", and "grid" technologies	kW	R^+	-
C^{el}	Cost of installation technologies for power supply where "el" refers to "PV", "wind", and "grid" technologies	USD	R^+	-
O^{el}	Cost of operation technologies for power supply where "el" refers to "PV", "wind", and "grid" technologies	USD/y	R^+	-
K_t	Electricity curtailed	kWh	R^+	$\forall\, t \in H$
Battery technology				
S_t	Battery State of Charge (SoC)	kWh	R^+	$\forall\, t \in H$
B_t	Electricity discharged (> 0) or charged (< 0) by the battery	kW	R	$\forall\, t \in H$
B^d_t	Electricity discharged by the battery	kW	R^+	$\forall\, t \in H$
B^c_t	Electricity charged by the battery	kW	R^+	$\forall\, t \in H$

β_t	Discharge (1), charge (0) mode selection	-	*{0,1}*	$\forall t \in H$
X	Installed battery capacity	kWh	R^+	-
$C^{battery}$	Cost of installation battery capacity	USD	R^+	-
$O^{battery}$	Yearly cost of operation battery	USD/y	R^+	-
Hydrogen storage technology				
T_t	Hydrogen storage level	kWh	R^+	$\forall t \in H$
H_t	Hydrogen discharged (> 0) or charged (< 0) by storage	kWh	R	$\forall t \in H$
Y	Installed hydrogen storage capacity	kWh	R^+	-
$C^{H2\text{-}storage}$	Cost of installation hydrogen storage capacity	USD	R^+	-
$O^{H2\text{-}storage}$	Yearly cost of operation hydrogen storage	USD/y	R^+	-
Electrolyzer technology				
F_t	Hydrogen produced from the electrolyzer	kWh_{H2}	R^+	$\forall t \in H$
E_t	Electricity consumed by the electrolyzer	kWh	R^+	$\forall t \in H$
Z	Installed electrolyzer capacity	kWh	R^+	-
$C^{electrolyzer}$	Cost of installation electrolyzer capacity	USD	R^+	-
$O^{electrolyzer}$	Yearly cost of operation electrolyzer	USD	R^+	-
Ammonia synthesis reactor				
Q_t	Ammonia produced from the synthesis reactor	kWh_{NH3}	R^+	$\forall t \in H$

R_t	Hydrogen feeding the ammonia synthesis reactor	kWh_{H2}	R^+	$\forall\, t \in H$
$C^{NH3\text{-}synthesis}$	Cost of installation of ammonia synthesis reactor	USD	R^+	-
$O^{NH3\text{-}synthesis}$	Yearly cost of operation ammonia synthesis reactor	USD/y	R^+	-
$D_t^{H3\text{-}synthesis}$	Electricity consumption of ammonia synthesis reactor	kWh	R	$\forall\, t \in H$
J	Installed capacity of ammonia synthesis reactor	USD	R^+	-
Air separation unit				
D_t^{ASU}	Electricity consumption of air separation unit	kWh	R	$\forall\, t \in H$
C^{ASU}	Cost of installation of air separation unit	USD	R^+	-
O^{ASU}	Yearly cost of operation air separation unit	USD/y	R^+	-
Total system				
C^{tot}	Total system cost of installation of system	USD	R^+	-
O^{tot}	Total system cost of operation	USD	R^+	-

S2.1.3 Parameters and input data

Table S3 details the parameters used in the formulation of the optimization model. Parameters' values can be year-, location-, and scenario-specific. Year-specific values are considered to account for cost-reduction, or efficiency-increase due to technological development. Location-

specific values are considered to account for the local renewable potential. Scenario-specific values, reported between brackets in **Table S3**, are considered to account for the parameter's possible range of variation.

Table S3. Parameters of the optimization model.

Symbol	Description	Values	Source
Power production technologies			
c^{PV}	Cost of installation of solar PV panels for power supply.	Year 2025: 1491.6 (1456.2, 1540.6) USD/kW Year 2045: 753.7 (602.7, 993.3) USD/kW	(NREL, 2024a) Utility-scale PV
c^{wind}	Cost of installation of wind turbines for power supply.	Year 2025: 1569 (1544, 1632) USD/kW Year 2045: 1188 (1093, 1411) USD/kW	(NREL, 2024a) Land-based wind turbines
c^{grid}	Cost of installation of grid connections for power supply.	0.0 USD/kW	-
o^{PV}	Operation and maintenance of solar PV panels for power supply.	Year 2025: 21.0 (20.6, 21.5) USD/kW/y Year 2045: 13.5 (11.8, 16.0) USD/kW/y	(NREL, 2024a) Utility-scale PV

o^{wind}	Operation and maintenance of wind turbines for power supply.	Year 2025: 31.3 (30.1, 31.9) USD/kW/y Year 2045: 26.3 (18.9, 29.1) USD/kW/y	(NREL, 2024a) Land-based wind turbines
o^{grid}	Operation and maintenance of grid connections for power supply.	0%	-
e^{grid}	Average business electricity retail price between 2023-2025	Country- dependent value (see Table 1)	(Global Petrol Prices, 2025)
η^c , η^d	Battery charge and discharge efficiencies	85%	(NREL, 2024a) Utility-scale battery
f^{PV}	Hourly local capacity factor PV panels	Time- and country-dependent value (see Table 1) Dataset MERRA-2 Global, 0.1 system loss fraction, 2-axis tracking system, 35 deg tilt, 180 deg azimuth.	(Pfenninger and Staffell, 2016)
f^{wind}	Hourly local capacity factor wind turbines	Time- and country-dependent value (see Table 1)	(Staffell and Pfenninger, 2016)

		Wind turbine model Vestas V150-4.5 MW, hub height of 105 m. Source: (Staffell and Pfenninger, 2016)	
Battery storage			
$b^{c,min}$ $b^{d,min}$	Minimum charging and discharging power compared to battery's rated capacity (kW)	0 kW 0 kW	This study
$b^{c,max}$ $b^{d,max}$	Maximum charging and discharging power as fraction of battery's rated capacity (kW)	100 % 100 %	This study
j^{min} j^{max}	Depth of discharge and the maximum battery state of charge as fraction of battery's rated capacity (kWh)	7% 100%	(Terlouw et al., 2022) This study
Δt	Time-step of battery power charging and discharging	1 hr	This study
$c^{battery}$	Cost of installation of battery	2025: 855.7 (695.4, 1080.0) USD/kWh 2045: 569.8 (425.5, 801.6)	(NREL, 2024a) Utility-scale battery

		USD/kWh	
$o^{battery}$	Cost for operation and maintenance	2.5 %/y of CapEx installation	(NREL, 2024a) Utility-scale battery
$m^{c,max}$ $m^{d,max}$	Maximum capacity allowed for installation	10 MWh	This study
□	Battery duration of charging/discharging at rated power	4 h	(NREL, 2024a) Utility-scale battery
Electrolyzer			
$\eta^{electrolyzer}$	Electrolyzer conversion efficiency	2025: 60.4% (51.4%, 69.5%) 2045: 71.7% (70.0%, 73.5%)	(Ueckerdt et al., 2021) (Everall and Everall, 2021)
$c^{electrolyzer}$	Cost of installation of electrolyzer	2025: 2474.4 (2243.7, 2705.2) USD/kW 2045: 710.1 (643.9, 776.3) USD/kW	2025: data from 2023 actualised to 2025 (IEA, 2024) 2050: (IEA, 2020) 2045: linear interpolation from 2025, 2050 data
$o^{electrolyzer}$	Cost for operation and	2% %/y of CapEx	(Terlouw et al.,

	maintenance of electrolyzer	installation	2022)
Hydrogen storage			
$c^{H2\text{-}buffer}$	Cost of installation of hydrogen buffer	2025: 653 (637, 669) USD/kWh_{H2} 2045: 241 (176, 307) USD/kWh_{H2}	(Terlouw et al., 2022)
$o^{H2\text{-}buffer}$	Cost for operation and maintenance	1 %/y of CapEx installation	(Terlouw et al., 2022)
Ammonia synthesis reactor			
$\eta^{NH3\text{-}synthesis}$	Stoichiometric hydrogen conversion into ammonia	88 %	(Smith et al., 2020)
□	Maximum relative variation of ammonia production within two following time-steps	15%	This study
$c^{NH3\text{-}synthesis}$	Cost of installation of ammonia synthesis reactor	40 USD/t_{NH3}	(Wang et al., 2021)
$o^{NH3\text{-}synthesis}$	Cost for operation and maintenance	2 %/y of CapEx installation	Assumed equal to electrolyzer
Ammonia demand			
d^{NH3}	Hourly ammonia demand	1 t_{NH3}/h	This study

S2.1.4 Constraints

Power supply

The supply of power is either from production from PV panels and wind turbines (autonomous system), purchased from the local grid (grid-connected system), or from a combination of the two systems (hybrid). P^{el}_t is the electricity produced in every time-step t based on production capacity W^{el}. Similarly, the cost of installation of the technologies for power production is defined by the sum of the cost of installation of PV panels and wind turbines, the cost of connection to the local grid, or a combination of both, here indicated at C^{el}, and O^{el} is the cost of operation.

Autonomous system

In the autonomous system, power production is a time- and space-dependent variable derived from the optimal PV panels and wind turbines capacity installed and the local capacity factor such that:

$$P_t^{el} = P_t^{PV} + P_t^{wind} - K_t \quad \text{(S3)}$$

where installed renewable power capacity (W^{PV}, W^{wind}) is derived from the hourly electricity produced and the local capacity factor:

$$P^{PV}_t = W^{PV} \cdot f_t^{PV} \quad \text{(S4)}$$

$$P_t^{wind} = W^{wind} \cdot f_t^{wind} \quad \text{(S5)}$$

where:

- P_t^{PV} (kWh): electric power production from PV panel at time t;
- P_t^{wind} (kWh): electric power production from wind turbines at time t;
- K_t (kWh): electric power curtailed at time t;
- W^{PV} (kW): installed capacity of PV panels;
- W^{wind} (kW): installed capacity of wind turbines;
- f_t^{PV} (-): local capacity factor[3] representative of the local generation profile of solar panels at time t;
- f_t^{wind} (-): local capacity factor representative of the local generation profile of wind turbines at time t.

The cost of installation is defined as:

$$C^{el} = C^{PV} + C^{wind} \quad \text{(S6)}$$

The cost of installation of PV panels and wind turbines is calculated as:

$$C^{PV} = c^{PV} \cdot W^{PV} \quad \text{(S7)}$$

$$C^{wind} = c^{wind} \cdot W^{wind} \quad \text{(S8)}$$

where:

- c^{PV} (USD/kW): cost of installation of PV panels;
- c^{wind} (USD/kW): cost of installation of wind turbines.

The cost of operation is defined as:

$$O^{el} = O^{PV} + O^{wind} \quad \text{(S9)}$$

The cost of operation and maintenance of PV panels and wind turbines is calculated as:

$$O^{PV} = o^{PV} \cdot W^{PV} \quad \text{(S10)}$$

$$O^{wind} = o^{wind} \cdot C^{wind} \quad \text{(S11)}$$

where:

- o^{PV} (USD/kW/y): operation and maintenance of PV panel;
- o^{wind} (%/y): operation and maintenance of wind turbines.

Grid-connected system

In the grid-connected system, all power is supplied from the grid, with no power curtailment:

$$P_t^{el} = P_t^{grid} \quad \text{(S12)}$$

where:

- P_t^{grid} (kWh): electric power production from PV panel at time t.

The cost of installation is defined as:

$$C^{el} = C^{grid} = c^{grid} \cdot W^{grid} \quad \text{(S13)}$$

where:

- c^{grid} (USD/kW): cost of grid connection.

The cost of operations is defined as:

$$O^{el} = O^{grid} = o^{grid} \cdot O^{grid} + \sum_{t \in H} (e^{grid} \cdot P_t^{grid}) \quad \text{(S14)}$$

where:

- o^{grid} (USD/kWh): operation and maintenance of grid connections;
- e^{grid} (USD/kWh): country-specific average electricity price.

Hybrid system

In the hybrid system, power can be supplied by three sources, and electricity produced from renewables can be curtailed:

$$P_t^{el} = P_t^{grid} + P_t^{PV} + P_t^{wind} - K_t \quad \text{(S15)}$$

Curtailment capacity ($W^{curtail}$) and grid import capacity (W^{grid}) are derived from the electricity curtailed and imported, and an 8760 h per year load factor:

$$W^{curtail} = (\sum_{t \in H} K_t) / 8760 \quad \text{(S16)}$$

$$W^{grid} = (\sum_{t \in H} P_t^{grid}) / 8760 \quad \text{(S17)}$$

where:

- $W^{curtail}$ (kW): curtailment capacity;
- W^{grid} (kW): installed capacity for power import from the grid.

The cost of installation is defined as:

$$C^{el} = C^{grid} + C^{PV} + C^{wind} \quad \text{(S18)}$$

The cost of operation and maintenance is defined as:

$$O^{el} = O^{grid} + O^{PV} + O^{wind} \quad \text{(S19)}$$

Battery

A battery storage system is expected to be included only in the case of power supply from renewable technologies, i.e., with an autonomous or hybrid system. The electricity charged or discharged from the electric battery is a time-dependent variable derived from the optimal

operation of the system to mitigate the impact of the intermittent production from PV panels and wind turbines on the operation of the downstream electrolyzer and ammonia synthesis reactor. The storage level of the battery at each time-step t is modeled in a linear form as:

$$S_t = S_{t-1} + \Delta t \left(B_t^c \ \eta^c - B_t^d \ / \eta^d \right) - S_{t-1} \ s^{sd} \quad \text{(S20)}$$

where:

- S_t, S_{t-1} (kWh): electricity stored in the battery at time (t) and (t-1);
- B^c_t, B^d_t (kW): electricity charge or discharge by the battery at each time step t;
- Δt (h): time-step of charge and discharge power;
- η^c, η^d: efficiencies while charging and discharging;
- s^{sd}: self-discharge loss as unit loss of stored energy per hour.

Electricity conservation over one year operation is enforced through the following constraint connecting the storage level at the first timestep of the year with the last timestep:

$$S_{(t = 8760)} = S_{(t = 1)} \quad \text{(S21)}$$

Additional constraints required to model the switch in charge-discharge operation modes are:

$$- (m^{c,max} / \boldsymbol{\tau}) (1 - \beta_t) \leq B_t^c \leq (m^{c,max} / \boldsymbol{\tau}) (1 - \beta_t) \quad \text{(S22)}$$

$$B_t - (m^{c,max} / \boldsymbol{\tau}) \beta_t \leq B_t^c \leq B_t + (m^{c,max} / \boldsymbol{\tau}) \beta_t \quad \text{(S23)}$$

$$- (m^{d,max} / \boldsymbol{\tau}) \beta_t \leq B_t^d \leq (m^{d,max} / \boldsymbol{\tau}) \beta_t \quad \text{(S24)}$$

$$B_t - (m^{d,max} / \boldsymbol{\tau})(1 - \beta_t) \leq B_t^d \leq B_t + (m^{d,max} / \boldsymbol{\tau}) (1 - \beta_t) \quad \text{(S25)}$$

- B_t (kW): electricity discharged (> 0) or charged (< 0) by the battery, equivalent to (B_t^d) and ($-B_t^c$) introduced as auxiliary variables to enable linear modeling of charge - discharge operation mode with different conversion efficiencies;
- β_t (-): binary variable indicating charging (0) or discharging (1) operation mode;
- $m^{c,max}$, $m^{d,max}$ (kWh): maximum capacity allowed for installation;
- □ (h): battery duration of charging/discharging at rated power, generally equal to 2 h, 4 h, or 6 h.

The minimum power operation in charging and discharging mode is introduced as:

$$b^{d,min} \beta_t \leq B_t^d \leq b^{d,max} (X / \square) \quad \text{(S26)}$$

$$b^{c,min} (1 - \beta_t) \leq B_t^c \leq b^{c,max} (X / \boldsymbol{\tau}) \quad \text{(S27)}$$

where:

- $b^{c,min}$, $b^{d,min}$ (kW): minimum charging and discharging power;
- $b^{c,max}$, $b^{d,max}$ (-): fractions of rated power defining maximum charging and discharging power;
- X (kWh): battery capacity.

Furthermore, the minimum and maximum battery's state of charge is defined based on the battery's rated power as:

$$j^{min} X \leq S_t \leq j^{max} X \quad \text{(S28)}$$

where:

- j^{min} , j^{max} (-): fractions defining minimum and maximum battery state of charge.

Additional details for accurate linear modeling of battery operations can be found in (Bracco et al., 2025).

The initial state of the battery is assumed to be equal to the state in the final time step within the set of timesteps *H* to allow the conservation of the power produced over the time steps considered in the optimization.

The cost of installation of the battery is calculated as:

$$C^{battery} = c^{battery} \cdot X \quad \text{(S29)}$$

where:

- $c^{battery}$ (USD/kWh): cost of installation of battery.

The cost of operation and maintenance of the battery, $O^{battery}$ (USD/y), is calculated as fraction of the cost of installation of the batteries:

$$O^{battery} = o^{battery} \cdot C^{battery} \quad \text{(S30)}$$

where:

- $o^{battery}$ (%/y): fraction of cost of installation for operation and maintenance.

Electrolyzer

The hydrogen produced from the electrolyzer is a time-dependent variable derived from the electricity consumed and the conversion efficiency such that:

$$F_t = \eta^{electrolyzer} \cdot E_t \quad (S31)$$

where:

- E_t (kWh): electricity feeding the electrolyzer;
- F_t (kWh): hydrogen produced from the electrolyzer;
- $\eta^{electrolyzer}$ (-): electrolyzer conversion efficiency.

The cost of installation of the electrolyzer is calculated as:

$$C^{electrolyzer} = c^{electrolyzer} \cdot Z \quad (S32)$$

where:

- $c^{electrolyzer}$ (USD/kW): cost of installation of electrolyzer;
- Z (kW): installed capacity of electrolyzer.

The cost of operation and maintenance of the electrolyzer, $O^{electrolyzer}$ (USD/y), is calculated as fraction of the cost of installation of the electrolyzer:

$$O^{electrolyzer} = o^{electrolyzer} \cdot C^{electrolyzer} \quad (S33)$$

where:

- $o^{electrolyzer}$ (%/y): fraction of cost of installation for operation and maintenance.

Hydrogen storage

Hydrogen storage is expected to be included only in the case of power supply from renewable technologies, i.e., with an autonomous or hybrid system. The hydrogen charged or discharged from the storage is a time-dependent variable derived from the optimal operation of the system to mitigate the impact of the intermittent production from PV panels on the operation of the downstream electrolyzer and ammonia synthesis reactor. The storage level of the buffer at each time-step t is computed as:

$$T_t = T_{t-1} - H_t \quad (S34)$$

where:

- T_t, T_{t-1} (kWh_{H2}): hydrogen stored in the buffer at time (t) and (t-1), with the assumption of empty buffer as initial state;
- H_t (kWh_{H2}): hydrogen discharge (> 0) or charge (< 0) by the storage at each time step t.

Hydrogen conservation over one year operation is enforced through the following constraint connecting the storage level at the first timestep of the year with the last timestep:

$$T_{(t = 8760)} = T_{(t = 1)} \quad \text{(S35)}$$

The total cost of installation of the hydrogen storage is calculated as:

$$C^{H2\text{-}buffer} = c^{H2\text{-}buffer} \cdot Y \quad \text{(S36)}$$

where:

- $C^{H2\text{-}buffer}$ (USD/kWh_{H2}): cost of installation of hydrogen buffer;
- Y (kWh_{H2}): installed hydrogen storage size.

The cost of operation and maintenance of the hydrogen buffer, $O^{H2\text{-}buffer}$ (USD/y), is calculated as fraction of the cost of installation of the hydrogen buffer:

$$O^{H2\text{-}buffer} = o^{H2\text{-}buffer} \cdot C^{H2\text{-}buffer} \quad \text{(S37)}$$

where:

- $o^{H2\text{-}buffer}$ (%/y): fraction of cost of installation for operation and maintenance.

Ammonia synthesis reactor

The ammonia produced from the ammonia synthesis reactor is a time-dependent variable derived from the hydrogen consumed its conversion efficiency such that:

$$Q_t = \eta^{NH3\text{-}synthesis} \cdot R_t \quad \text{(S38)}$$

where:

- R_t (kWh): hydrogen consumed from the ammonia synthesis reactor;
- Q_t (kWh_{NH3}): ammonia produced from the ammonia synthesis reactor;
- $\eta^{NH3\text{-}synthesis}$ (-): ammonia synthesis reactor conversion efficiency hydrogen to ammonia.

Due to the slow dynamics of the reactor, related to the temperature reaction, the rate of variation of the ammonia production is limited by the following constraints:

$$| Q_t - Q_{t-1} | / Q_{t-1} \leq \delta \quad \text{(S39)}$$

where:

- δ (%): maximum relative variation of ammonia production within two following time-steps.

It should be noted that the imposed maximum rate of variation of ammonia production significantly affects the role of electricity and hydrogen storage in mitigating the intermittency of PV panels and wind turbines.

The cost of installation of the reactor is calculated as:

$$C^{NH3\text{-}synthesis} = c^{NH3\text{-}synthesis} \cdot J \quad \text{(S40)}$$

where:

- $c^{NH3\text{-}synthesis}$ (USD/kW_{NH3}): cost of installation of ammonia synthesis reactor;
- J (kW_{NH3}): installed capacity of ammonia synthesis reactor.

The cost of operation and maintenance of the ammonia synthesis reactor, $O^{NH3\text{-}synthesis}$ (USD/y), is calculated as fraction of the cost of installation of the ammonia synthesis reactor:

$$O^{NH3\text{-}synthesis} = o^{NH3\text{-}synthesis} \cdot C^{NH3\text{-}synthesis} \quad \text{(S41)}$$

where:

- $o^{NH3\text{-}synthesis}$ (%/y): fraction of cost of installation for operation and maintenance.

Energy balance

The energy balance constraints are introduced for every energy carrier considered. For electricity, the energy balance is imposed at every hour t as:

$$P^{el}_t + B_t - E_t - K_t = D_t^{ASU} + D_t^{NH3\text{-}synthesis} \quad \text{(S42)}$$

where:

- D^{ASU} (kWh): electricity consumption Air Separation Unit at time step t;
- $D^{NH3\text{-}synthesis}$ (kWh): electricity consumption ammonia synthesis reactor at time step t.

For hydrogen, the energy balance is imposed at every hour t as:

$$F_t + H_t - R_t = 0 \quad \text{(S43)}$$

For every subset of timesteps H_s ($s \in S$) the ammonia production from the reactor is imposed to equal the sum of ammonia demand within the subset of timesteps H_s such that:

$$\sum_{t \in Hs} Q_t = \sum_{t \in Hs} d_t^{NH3} \quad \text{(S44)}$$

where:

- $\sum_{i \in Hs} d_i^{NH3}$ is the demand for ammonia within the subset of timesteps H_s;
- $H_1 \cup ... \cup H_s \cup ... \cup H_S$ is equivalent to the set of timesteps H representative of the 8760 hours in a year.

The number of timesteps within H_s is assumed to equal 720 hours for every subset $s \in S$. The choice of 720 hours as size of each subset H_s is assumed as a compromise between predictability of production over time and system flexibility to accommodate for the intermittency and variability of power production from renewable technologies.

Total system cost

The total capital expenditure of the system (C^{tot} (USD)) includes the cost of installation of each component, described in the following:

$$C^{tot} = C^{el} + C^{battery} + C^{electrolyzer} + C^{H2\text{-}buffer} + C^{NH3\text{-}synthesis} + C^{ASU} \quad \text{(S45)}$$

The yearly total operating expenditure of the system (O^{tot} (USD/y)) includes the operations and maintenance of each component, described in the following:

$$O^{tot} = O^{el} + O^{battery} + O^{electrolyzer} + O^{H2\text{-}buffer} + O^{NH3\text{-}synthesis} + O^{ASU} \quad \text{(S46)}$$

S3. Local sensitivity analysis

The MILP model is presented in Section **S2. System optimization model** is here converted into a linear problem (LP) to run a local sensitivity analysis of key decision variables and parameters, affected by location-specific conditions, which significantly affect the LCOA.

Variables to parameters

Some of the decision variables from the MILP model are converted into controlled parameters of the LP model:

- X (kWh): battery capacity;
- Y (kWh_{H2}): installed hydrogen storage size;
- $\sum_{t \in H} K_t$ (kWh): total curtailment over the year.

While defining these variables requires an hourly resolution model, in the LP model they are assumed as exogenous parameters of the optimization problem. Since the integer variables of the MILP were all related to the operation of the battery, removing the constraints which define the hourly battery operation makes the problem linear.

Model formulation

With the conversion of storage capacity sizing variables into exogenous parameters, and the removal of the integer variables describing the operation of the battery, all the decision variables are linear decision variables. Additionally, the time resolution of the problem is converted from hourly- into yearly-resolution. All the decision variables, defined over timesteps $t \in H$**,** are scalar decision variables here. Accordingly, all the hourly energy fluxes in the mass balance constraints become yearly energy fluxes.

Input data

Data used for the sensitivity analysis consists of a reference medium scenario for input parameters of the optimization model, a set of parameters derived from the results of this study and used to control some of the decision variables of the optimization problem, and a range of variation for the key parameters varied within the sensitivity analysis.

Table S4. Parameters and data input of the sensitivity analysis. Rows in *italic* highlight the decision variables treated as constant parameters, i.e., variables whose value has been set with an equality constraint within the sensitivity analysis. Values of range of variation are derived from parameters in **Table S3** or from the results presented in the main article.

Parameter	Medium scenario - 2035	Range of variation
cost of capital, r	6.6 %	(4.3, 11.6) %
Power production technologies		
PV CapEx, c^{PV}	895.3 USD/kW	(602.7, 1540.6) USD/kW
wind CapEx, c^{wind}	1334 USD/kW	(1093, 1632) USD/kW
grid CapEx, c^{grid}	0.0 USD/kW	-
PV OpEx, o^{PV}	15 USD/kW/y	-
wind OpEx, o^{wind}	28 USD/kW/y	-
grid OpEx, o^{grid}	0%	-
c.f. PV, f^{PV}	22.8%	(19.2, 26.4) %
c.f. wind, f^{wind}	34.1%	(17.5, 50.6) %
total curtailment, K	*20 GWh*	*(0, 30) GWh*
Battery storage		
battery CapEx, $c^{battery}$	674	(425, 1080) USD/kWh
battery OpEx, $o^{battery}$	2.5 %/y of CapEx installation	-
battery capacity, X	*10 MWh*	*(5, 15) MWh*

Electrolyzer		
eff. electrol., $\eta^{electrolyzer}$	67.1 %	-
CapEx electrol., $c^{electrolyzer}$	1592	(644, 2705) USD/kW
OpEx electrol.,$o^{electrolyzer}$	2% %/y of CapEx installation	-
Hydrogen storage		
CapEx H_2 storage, $c^{H2\text{-}buffer}$	13 USD/kWh_{H2}	(10.5, 20) USD/kWh_{H2}
OpEx H_2 storage, $o^{H2\text{-}buffer}$	1 %/y of CapEx installation	-
H_2 storage size, Y	*300 MWh*	*(100, 500) MWh*
Ammonia synthesis reactor		
eff. NH_3 reactor, $\eta^{NH3\text{-}synthesis}$	88 %	-
CapEx NH_3 reactor, $c^{NH3\text{-}synthesis}$	40 USD/t_{NH3}	-
OpEx NH_3 reactor, $o^{NH3\text{-}synthesis}$	2 %/y of CapEx installation	-
Ammonia demand		
ammonia demand d^{NH3}	1 t_{NH3}/h	-

S4. Ammonia demand in selected countries

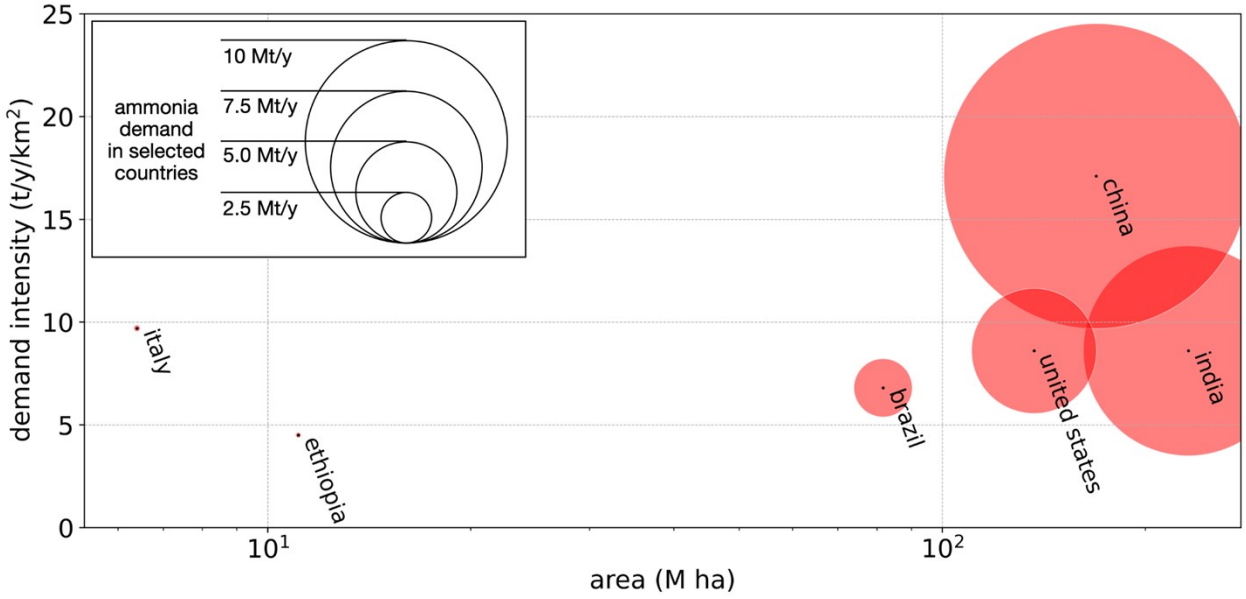

Figure S1. Ammonia demand in selected countries. The figure classifies countries based on cropland area (x-axis, log-scale), demand intensity (y-axis), and total demand of ammonia for use as nitrogen fertilizer on croplands. Demand intensity corresponds to the nutrient demand by crops per unit of harvested area. Original data source representative of nitrogen demand as crop nutrient in 2020 (Adalibieke et al., 2023).

Table S5. Ammonia demand distribution by country. The table reports the demand of ammonia as fertilizer for crop production in the selected countries. Key statistics describing demand intensity and distribution are reported. Original data source representative of nitrogen demand as crop nutrient in 2020 (Adalibieke et al., 2023).

Brazil Total demand: 5.5 Mt/y Total cropland area: 81.7 M ha Avg. demand rate: 6.8 t/y/km^2 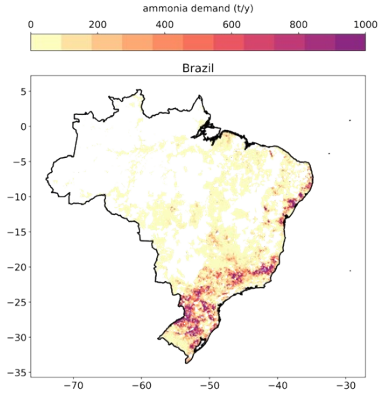	**China** Total demand: 28.8 Mt/y Total cropland area: 169.1 M ha Avg. demand rate: 17.1 t/y/km^2 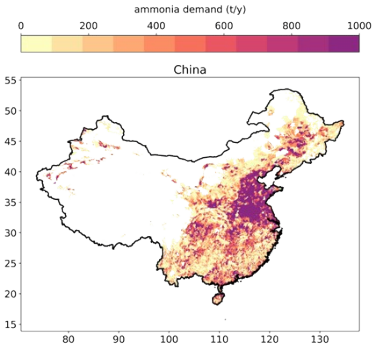	**Ethiopia** Total demand: 0.5 Mt/y Total cropland area: 11.1 M ha Avg. demand rate: 4.5 t/y/km^2 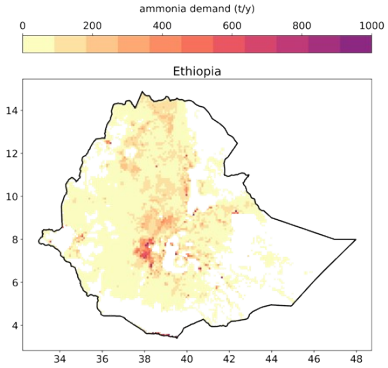
India Total demand: 19.8 Mt/y Total cropland area: 231.5 M ha Avg. demand rate: 8.6 t/y/km^2	**Italy** Total demand: 0.6 Mt/y Total cropland area: 6.4 M ha Avg. demand rate: 9.7 t/y/km^2	**United States** Total demand: 11.8 Mt/y Total cropland area: 136.8 M ha Avg. demand rate: 8.6 t/y/km^2

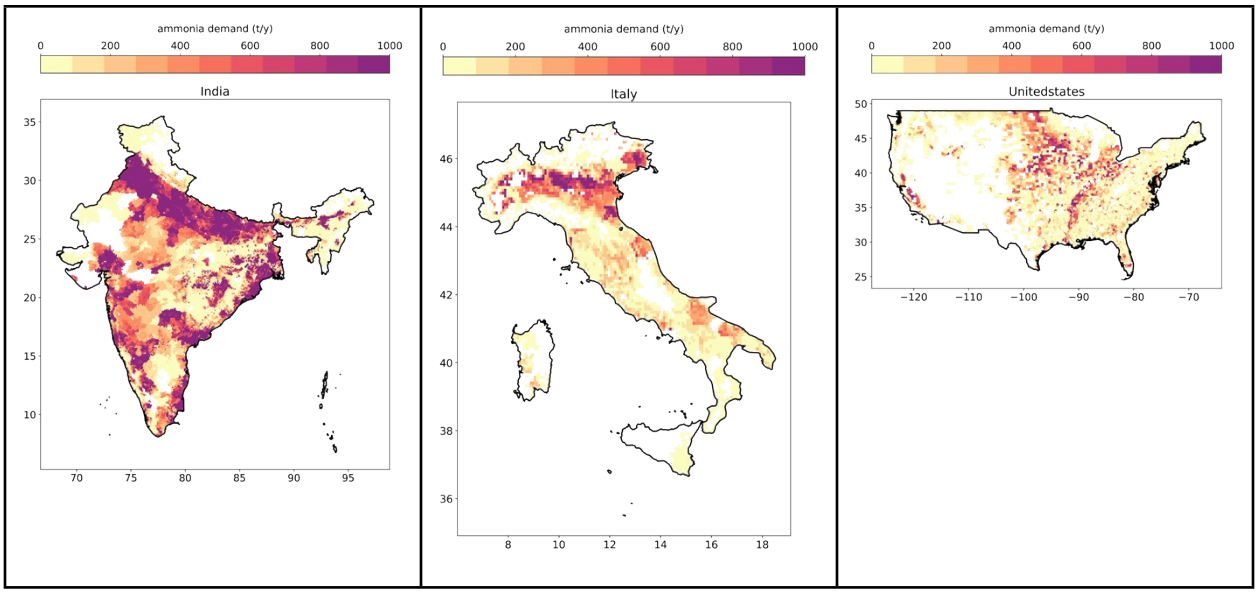
ammonia demand (t/y)
0
200
400
600
800
1000
India
35
30
25
20
15
10
70
75
80
85
90
95
ammonia demand (t/y)
0
200
400
600
800
1000
Italy
46
44
42
40
38
36
8
10
12
14
16
18
ammonia demand (t/y)
0
200
400
600
800
1000
Unitedstates
50
45
40
35
30
25
−120
−110
−100
−90
−80
−70

S5. Design scenarios comparison

Annualized CapEx

To compare the investment in technologies installed with the yearly cost of electricity consumption from the grid, the CapEx is presented as annual cost over the plant lifetime:

$$\text{Annualized CapEx} = \text{CapEx} \cdot r / (1 - (1 + r)^{-T}) \quad \text{(S48)}$$

where:

- Annualized CapEx (USD/y): equivalent annual cost of CapEx over plant lifetime;
- CapEx (USD): capital expenditure for installation of plant's components;
- r: cost of capital;
- T: plant's lifetime.

Design scenarios comparison

The following tables collect the results of the year- and cost-scenarios not presented in the figures of the main article (**Section 4.1**).

Table S6. Annual cost of power production technologies in different system configurations, year- and cost-scenarios. The three bars for each country correspond to the three system configurations considered: (left) autonomous, (center) hybrid, (right) grid-connected.

legend	ann. CapEx PV; ann. CapEx wind; O&M PV; O&M wind; import grid	
year	**2025**	**2045**
scenario		
low	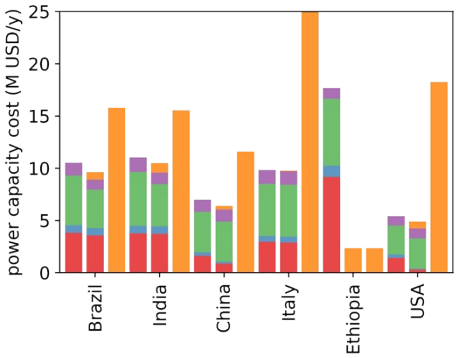	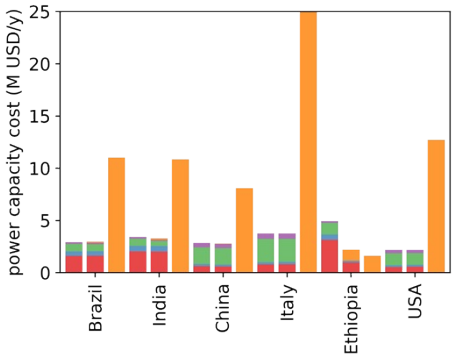
high	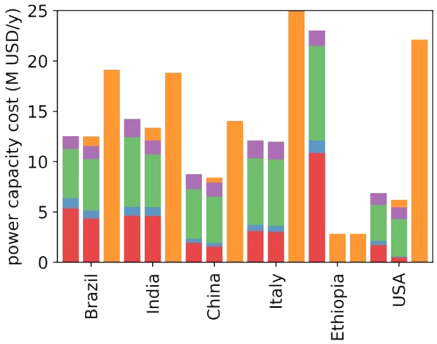	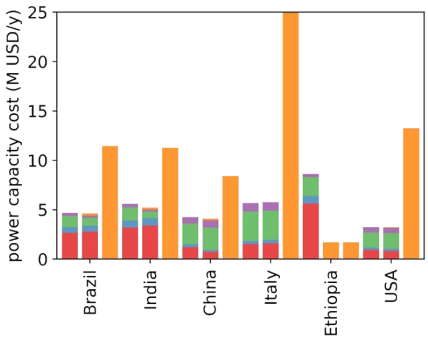

Table S7. Annual cost of storage technologies in different system configurations, year- and cost-scenarios. The three bars for each country correspond to the three system configurations considered: (left) autonomous, (center) hybrid, (right) grid-connected.

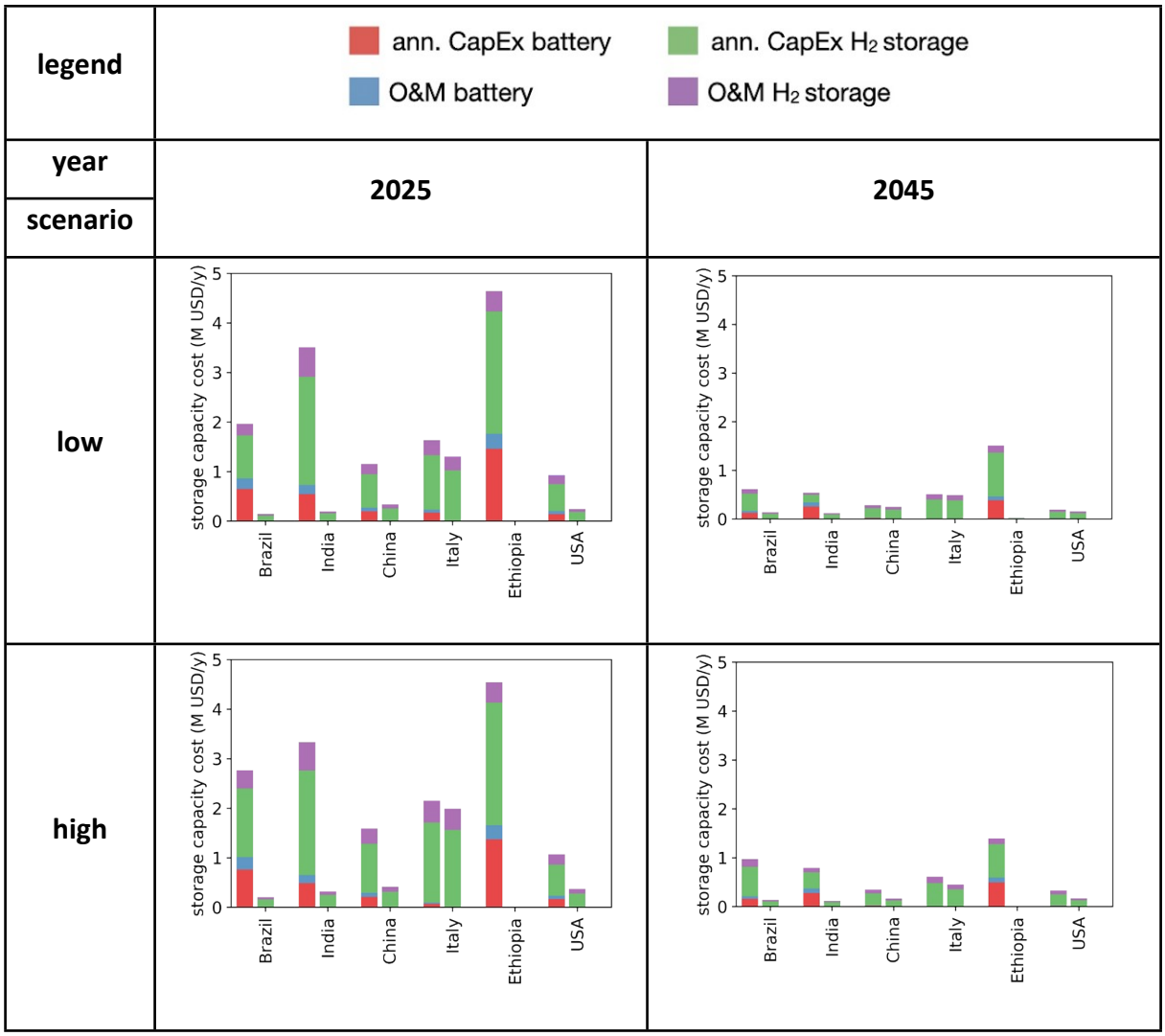

Table S8. Components' design: power production in different system configurations, year- and cost-scenarios. The three bars for each country correspond to the three system configurations considered: (left) autonomous, (center) hybrid, (right) grid-connected.

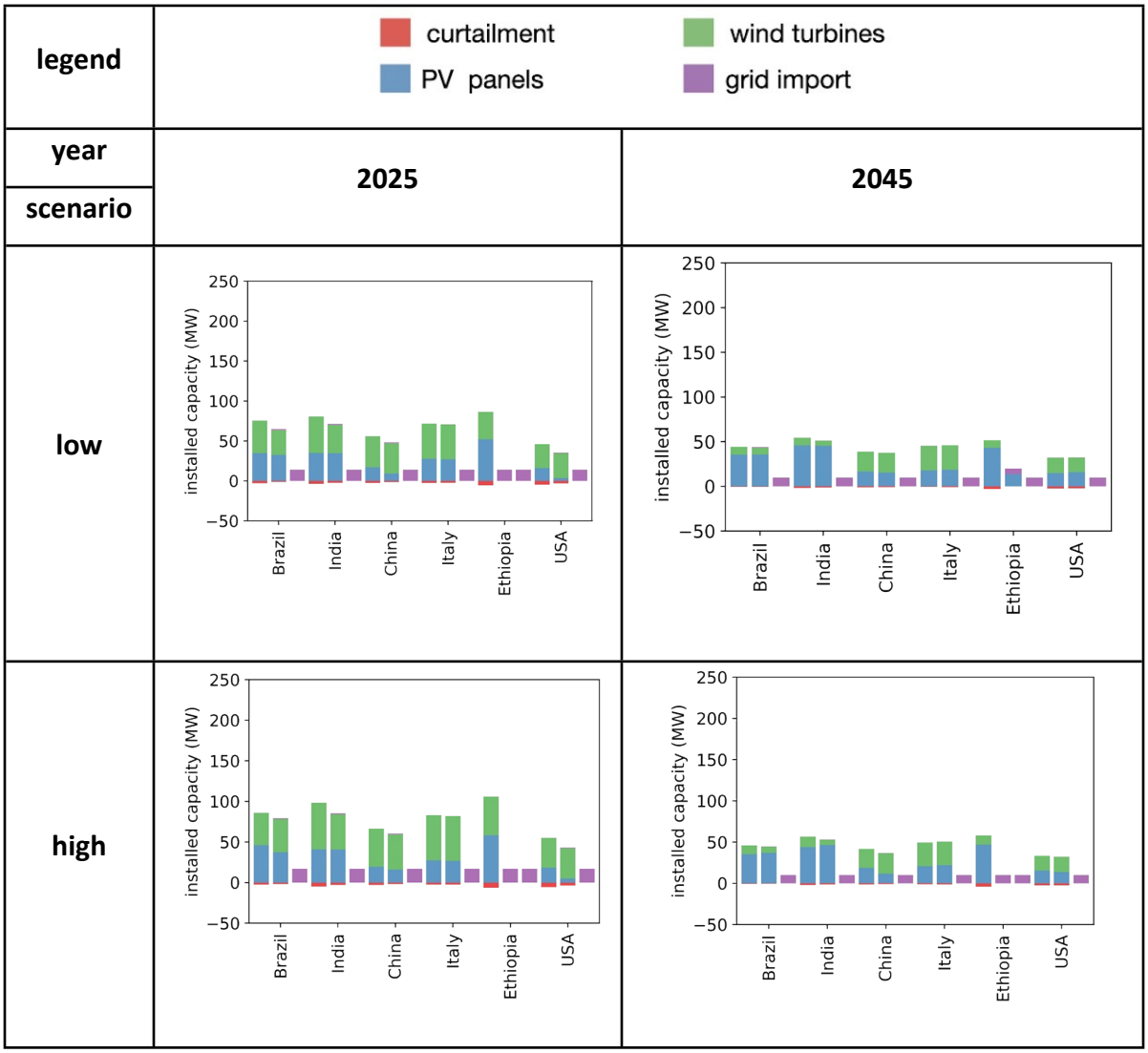

Table S9. Storage capacities in different system configurations, year- and cost-scenarios. The three bars for each country correspond to the three system configurations considered: (left) autonomous, (center) hybrid, (right) grid-connected.

legend	battery, H_2 storage	
year	2025	2045
scenario		
low	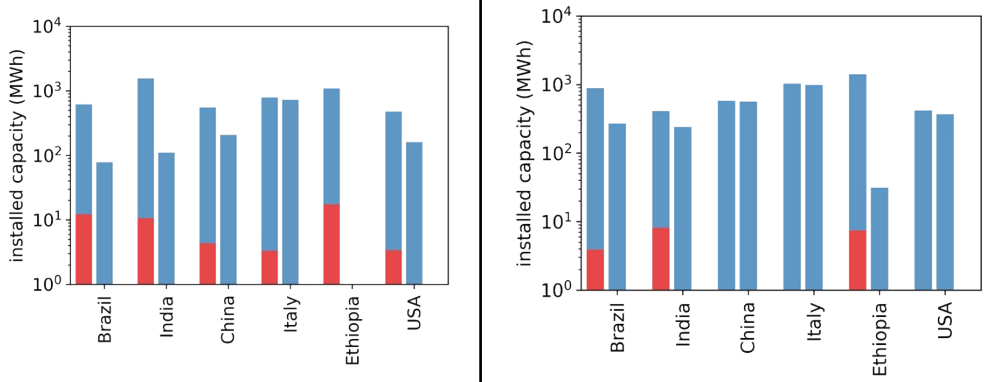	
high	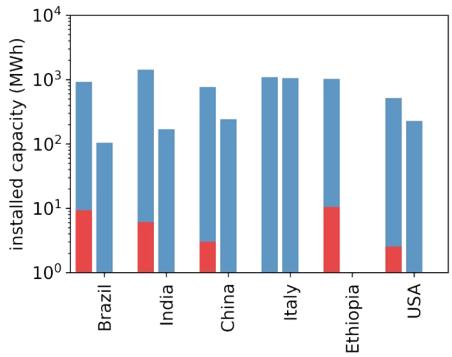	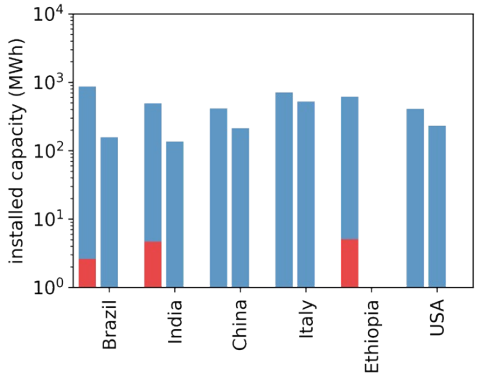

Supplementary References

Gurobi Optimization, LLC, 2025. Gurobi Optimizer Reference Manual. https://www.gurobi.com

Garcia, S., Bracco, S., Parejo, A., Fresia, M., Guerrero, J.I. and Leon, C., 2025. Cost-Effective Operation of Microgrids: A MILP-Based Energy Management System for Active and Reactive Power Control. International Journal of Electrical Power & Energy Systems, 165, p.110458.

Damodaran, A., 2023. Equity Risk Premiums (ERP): Determinants, Estimation and Implications - The 2023 Edition. http://dx.doi.org/10.2139/ssrn.4398884

Damodaran A., 2025. Global Cost of equity and capital in US dollars - data updated on 05/01/2025. Contacts: Aswath Damodaran, adamodar@stern.nyu.edu. Database last access 28/07/2025. Website: http://www.damodaran.com

Ueckerdt, F., Bauer, C., Dirnaichner, A., Everall, J., Sacchi, R. and Luderer, G., 2021. Potential and risks of hydrogen-based e-fuels in climate change mitigation. Nature Climate Change, 11(5), pp.384-393.

Everall, J. & Ueckerdt, F. Electrolyser CAPEX and efficiency data for: potential and risks of hydrogen-based e-fuels in climate change mitigation. Version 1 (Zenodo, 2021); https://doi.org/10.5281/ZENODO.4619892

National Renewable Energy Laboratory (NREL). 2024a. 2024 Annual Technology Baseline. Golden, CO: National Renewable Energy Laboratory. https://atb.nrel.gov/

National Renewable Energy Laboratory (NREL). Badgett, A., Brauch, J., Thatte, A., Rubin, R., Skangos, C., Wang, X., Ahluwalia, R., Pivovar, B. and Ruth, M., 2024b. Updated Manufactured Cost Analysis for Proton Exchange Membrane Water Electrolyzers. Golden, CO: National Renewable Energy Laboratory. NREL/TP-6A20-87625.

Pfenninger, S., and Staffell, I., 2016. Long-term patterns of European PV output using 30 years of validated hourly reanalysis and satellite data. Energy 114, pp. 1251-1265.

Staffell, I., and Pfenninger, S., 2016. Using Bias-Corrected Reanalysis to Simulate Current and Future Wind Power Output. Energy, 114, 1224–1239. Website: http://dx.doi.org/10.1016/j.energy.2016.08.068

International Energy Agency (IEA), 2024. Global Hydrogen Review 2024. https://www.iea.org/reports/global-hydrogen-review-2024

International Energy Agency (IEA), 2020. Global average levelised cost of hydrogen production by energy source and technology, 2019 and 2050. https://www.iea.org/data-and-statistics/charts/global-average-levelised-cost-of-hydrogen-production-by-energy-source-and-technology-2019-and-2050

Terlouw, T., Bauer, C., McKenna, R. and Mazzotti, M., 2022. Large-scale hydrogen production via water electrolysis: a techno-economic and environmental assessment. Energy & Environmental Science, 15(9), pp.3583-3602.

Smith, C., Hill, A.K. and Torrente-Murciano, L., 2020. Current and future role of Haber–Bosch ammonia in a carbon-free energy landscape. Energy & environmental science, 13(2), pp.331-344.

Wang, M., Khan, M.A., Mohsin, I., Wicks, J., Ip, A.H., Sumon, K.Z., Dinh, C.T., Sargent, E.H., Gates, I.D. and Kibria, M.G., 2021. Can sustainable ammonia synthesis pathways compete with fossil-fuel based Haber–Bosch processes?. Energy & Environmental Science, 14(5), pp.2535-2548.